Supplemental information

A. Blade geometry

The sharpness of razor blades used in this study (#27-251, Razor Blade Company, Van Nuys, CA) was characterized by imaging the tip of a fresh, untouched blade using a SEM (Zeiss LEO 1550 FESEM, Oberkochen, Germany). As shown in Supplemental Figure 1, the radius at the tip of these uncoated blades is approximately 75 nm and the apex angle at the tip is 29° ± 1°, as measured using ImageJ.

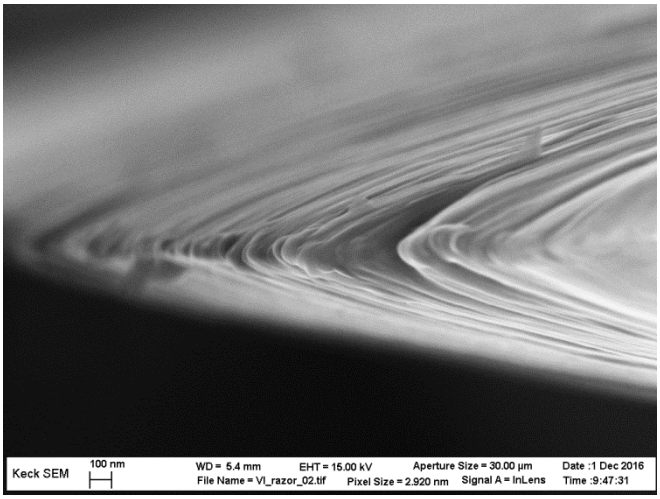

Supplemental Figure 1. A SEM image showing the tip of a fresh razor blade. The radius of the tip is approximately 75 nm.

B. Mixed-effect linear models of bulk responses

Critical bulk force, blade depth and integrated energy at the point of first fracture were fit to mixed-effects linear regression models in order to test for significant effects. Each of these three responses was fit to a linear model which included all individual and interaction terms for the available variables: sample orientation (parallel or perpendicular to the split-line), surface condition (intact or removed), storage time between dissection and testing, source condyle (medial or lateral), and the natural log of the blade speed. A random effect was added to account for samples that originated from different animals. These models were implemented in MATLAB (The MathWorks Inc, Natick, MA) using the `fitlme` function. Each full model was reduced by iteratively removing

insignificant highest-order terms ($p > 0.01$) and fitting again, using the Satterthwaite approximation for computing degrees of freedom. The residuals of each model were also checked for normality and homogeneity.

Response = A + B × ln(blade speed)	Parameter A			Parameter B		Goodness of fit
	Parameter value		p-value	Parameter value	p-value	Adjusted R^2
	Intact	Removed	Intact vs. Removed	Intact or Removed	Value vs. zero	
Cut force (N)	0.484	0.462	0.96	−0.0242	2.6×10^{-5}	0.12
Cut depth (μm)	293	162	1.2×10^{-29}	−24.5	5.5×10^{-21}	0.72
Cut energy (μJ)	42.3	34.2	1.7×10^{-4}	−4.87	6.1×10^{-16}	0.42

Supplementary Table 1. Coefficients, significance values, and goodness of fit values for the reduced mixed-effects linear models of critical bulk force, depth, and energy at first cut, and the toughness (throughout cutting) as shown in Figure 2B-D. In all cases, the full model was reduced by removing insignificant higher-order fixed effects ($p > 0.01$), resulting in the final two-parameter model shown here.

C. Strain energy density spatial extent

The spatial extent of individual strain energy fields in undeformed coordinates was characterized by taking the lateral- and depth-variance of data points above a strain-energy threshold of 20 KJ/m^3. Each variance was then fit to a reduced, fixed-effects linear model to test for significant effects. Each linear model included all individual and interaction terms for the available variables: sample orientation (parallel or perpendicular to the split-line), surface condition (intact or removed), storage time between dissection and testing, source condyle (medial or lateral), and the natural log of the blade speed. These models were implemented in MATLAB using the `fitlm` function. Each full model was reduced by iteratively removing insignificant highest-order terms ($p > 0.01$) and fitting again, using the Satterthwaite approximation for computing degrees of freedom. The residuals of each model were also checked for normality and homogeneity.

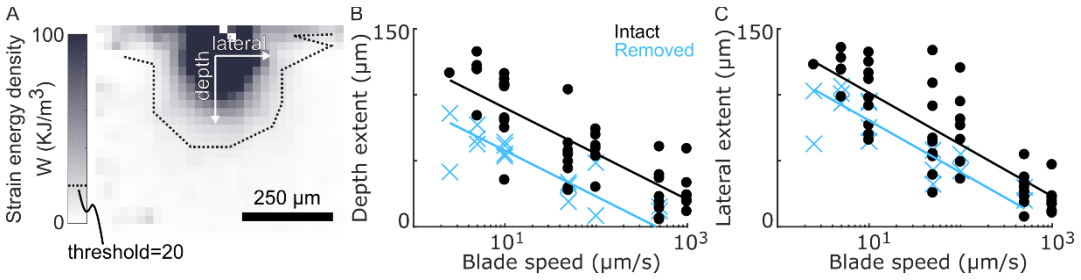

Supplemental Figure 2. Analysis of the spatial extent of the strain energy density field in the lateral and depth dimensions. (A) Example strain energy density field showing the points above the threshold value of 20 KJ/m^3. Points above this threshold were analyzed to calculate the variance in the (B) depth and (C) lateral directions for surface-intact samples (black circles) and surface-removed samples (blue circles). This data was fit to a fixed-effects model based on the log of the blade speed and the surface condition and these fits are shown as solid lines. The fits are further detailed in Supplementary Table 2.

Response = A + B × ln(blade speed)	**Parameter A**			**Parameter B**		**Goodness of fit**
	Parameter value		p-value	Parameter value	p-value	Adjusted R^2
	Intact	Removed	Intact vs. Removed	Intact or Removed	Value vs. zero	
Depth extent (μm)	125	92.4	3.3 E -7	-15.1	3.0 E -17	0.69
Lateral extent (μm)	141	120	1.4 E -3	-17.0	1.7 E -17	0.68

Supplementary Table 2. Coefficients, significance values, and goodness of fit values for the linear fixed-effects models of the lateral and depth extent of the strain energy fields, as shown in Supplemental Figure 2B-C.

D. Radial displacement fields fits

In order to compare observed sample deformation with that predicted by contact mechanics, local 2D displacement data was fit to the 2D functional form predicted by contact mechanics (Johnson, 1987). Although this theory assumes infinitely-sharp indentation of a Hookean elastic half space under small strain conditions, Equation 2 fit the data reasonably well, as shown in Figure 6. To highlight the logarithmic scaling, data and fits were scaled by the fitting parameters, β_i, and these 1D cuts of the normalized 2D data and fits are shown on a linear-log plot in Supplemental Figure 3.

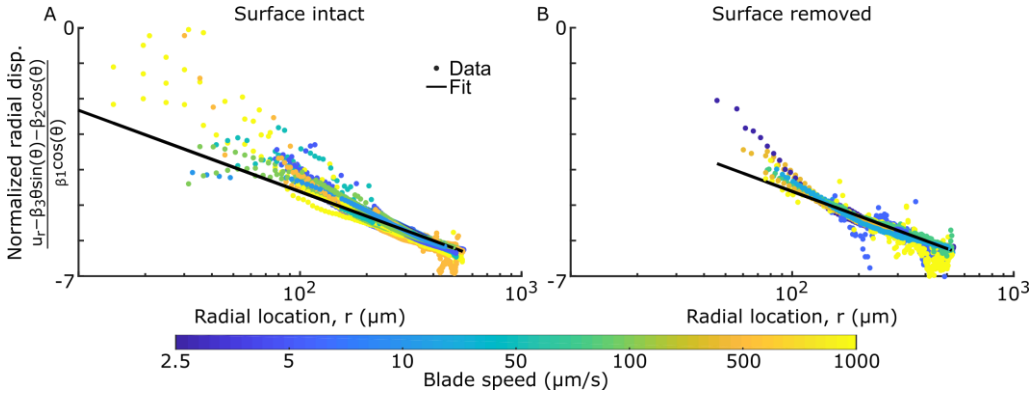

Supplemental Figure 3. Cuts of the 2D displacement data and associated 2D fits to the functional form predicted by contact mechanics. Data and fits are shown for (A) surface-intact and (B) surface-removed samples, with cuts take at θ = 0°. The data and fits were scaled based on the fitting parameters and are shown on a linear-log plot to emphasize the collapse and logarithmic scaling of the data. Note, this is the same data as shown in Figure 6, but scaled.

It is also interesting to inspect the values of the fitting coefficients obtained from these fits (β_i in Equation 2). Although β_2 is difficult to interpret due to the unknown influence of the scaling constant (*R*), fitted values for β_1 and β_3 can be directly calculated by assuming reasonable values of the Poisson's radio, ν, and Young's modulus, *E*, taken from the literature and values of $P = F_C/(3\text{ mm})$ from this study. Assuming $\nu \approx 0.0$ to 0.5, $E \approx 1$ to 50 MPa, and $F_C \approx 0.5$ to 0.9 N, we expect $\beta_1 \approx 1$ to 200 μm and $\beta_3 \approx 0$ to 100 μm. The actual coefficients for β_1 and β_3 did agree with the expected values, as summarized in Supplementary Table 3 and Supplemental Figure 4. Note that, on average, values for β_1 and β_3 were higher for surface-intact samples, which is expected since the modulus of the surface layer is smaller and β_1 and β_3 are both inversely proportional to *E*. Alternatively, β_1 and β_3 can be used to calculate E and ν, resulting in values shown in Supplemental Figure 5. Again, these values lie in the ranges expected for articular cartilage. Also note that that the Young's modulus for surface-intact samples is slightly lower than surface-removed, as would be expected due to the influence of the compliant surface layer.

	Surface intact			**Surface removed**		
	β_1	**β_2**	**β_3**	**β_1**	**β_2**	**β_3**
Mean (μm)	42.3	330	20.0	16.7	164	5.27
Standard error (μm)	4.9	33	1.8	2.9	19	1.1

Supplementary Table 3. Fit coefficients for surface-intact and surface-removed samples obtained by fitting local displacement data to Equation 2 in a 2D, least-squares sense. For each coefficient, the average value and the standard error of the mean are shown.

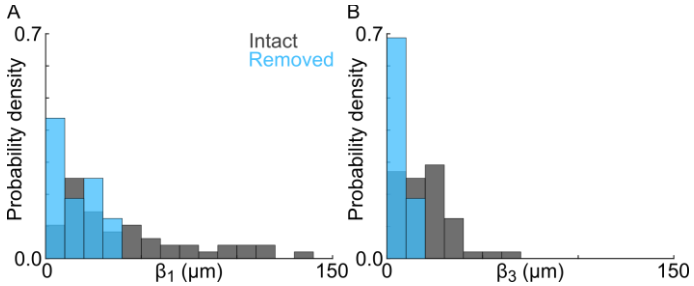

Supplemental Figure 4. Histograms of the fit coefficients (A) β_1 and (B) β_3 obtained by fitting local displacement data to Equation 2. Note that, the values lie in the expected range of values and values for surface-intact samples are generally higher than surface-removed.

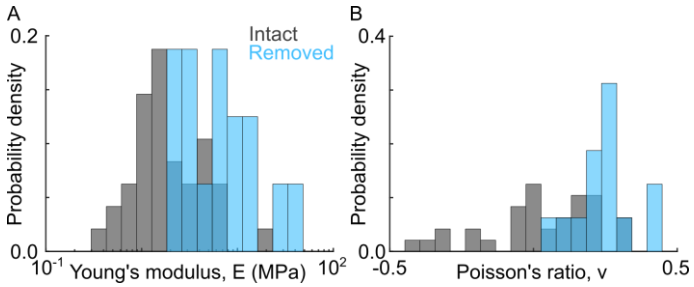

Supplemental Figure 5. Histograms of the (A) Young's modulus and (B) Poisson's ratio calculated from the) β_1 and β_3 fitting coefficients. Note that, the values lie in the expected ranges for articular cartilage and surface-removed values are generally higher than surface-intact.

E. Toughness calculation

In the current study, the primary focus was on damage initiation in articular cartilage. However, the propagation of existing cracks is also an important and understudied issue relevant to articular cartilage. A handful of studies have applied traditional and more novel fracture tests to characterize the toughness of articular cartilage and other soft biomaterials (Chin-Purcell and Lewis, 1996; Simha et al., 2003; Stok and Oloyede, 2007; Taylor et al., 2012). When characterizing this crack propagation, many studies extract a measure of the toughness material property, or the ability of the material to resist cracking, based on the strain energy release rate (i.e. energy released per crack area). These existing studies observed toughness values from

140 J/m^2 to over 1000 J/m^2 for articular cartilage. Although not the main focus of the present study, the bulk data after the first-cut provides a window to explore crack propagation in our system.

To estimate a measure of toughness from the present study, we analyzed the bulk force-displacement data after the first-cut, i.e. during the sawtooth-region. In particular, we anticipate that a taller and wider sawtooth implies a tougher material, since the energy build-up and loss during this time should reflect the strain energy released to create the new crack surface. To isolate these regions of strain build-up, the derivative of the force was thresholded to determine points during energy build-up (i.e. with positive slope) and only these areas were integrated, as depicted in Supplemental Figure 6A. This energy was then divided by the final crack area, as determined by confocal images taken after each experiment (depth- and surface-profiles). This toughness measure was fit to a reduced mixed-effects linear model to determine significant effects with a random effect for animal, following the same procedure for linear models of the cut force, depth, and energy (as described in the "Methods", "Data analysis" subsection and shown in Figure 2B-D). Note that this measure of toughness effectively excludes the first-cut. Based on the confocal videos, we estimate this first cut to be about 10 – 50 μm deep in undeformed coordinates. Instead, this measure of toughness applies to the tissue depth from after this first cut through the final cut depth, which is usually many-hundred microns. As such, the toughness comparison measure does not apply to the most superficial ~50 μm and is also likely a slight underestimation of the full value.

The results of this toughness measure are shown in Supplemental Figure 6B as a function of surface condition and blade speed. As with the other bulk results (Figure 2B-D, Supplementary Table 1), these were the only two significant factors in the linear model (Supplementary Table 4). Averaged across blade speed, the toughness was 32.3 J/m^2 for surface-intact samples and 68.0 J/m^2 for surface-removed samples.

These results suggests that (after the first 20-50 μm) toughness increases with depth into the tissue. As mentioned previously in the "Discussion" section, it is especially interesting to note that our measure of toughness is closest to that measured by Chin-Purcell and Lewis (1996). This study measured a toughness of

140 J/m^2 for their most brittle-like samples and this brittle-like fracture is most comparable to the experimental system used in this study. However, in both surface-intact and surface-removed samples, our measure of toughness is lower than those reported elsewhere in the literature, which may reflect limitations of the current calculation. This measure of toughness also has a slight dependence on blade speed. Since toughness is a material property, this rate dependence is non-ideal and may reflect time-dependent strain relaxation and energy dissipation in the tissue that is not appropriately incorporated into the current calculation.

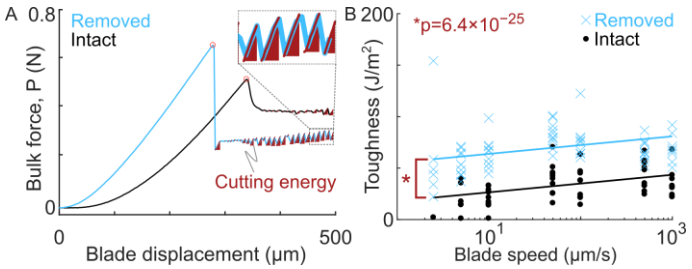

Supplemental Figure 6. (A) Characteristic force vs. blade displacement curves for one surface-intact and one surface-removed sample, up to the blade turn-around point. Both samples were taken from the 10 μm/s blade speed group and are the same samples shown in Figure 2A. For all samples, the energy expended during the full cutting time was integrated, as depicted by red areas. This energy was divided by the final cut area as a measure of toughness. (B) The toughness for all experiments (circles or crosses), shown with the corresponding reduced linear model fits (solid lines), for surface-intact (black) and surface-removed (blue) samples. This measure of toughness was significantly dependent on blade speed (p-value: 3.1×10^{-5}) and surface condition, with surface-removed having a higher toughness (p-value: 6.4×10^{-25}).

Response = A + B × ln(blade speed)	**Parameter A**			**Parameter B**		**Goodness of fit**
	Parameter value		p-value	Parameter value	p-value	Adjusted R^2
	Intact	Removed	Intact vs. Removed	Intact or Removed	Value vs. zero	
Toughness (J/m^2)	54.9	17.6	6.4×10^{-25}	3.71	3.1×10^{-5}	0.64

Supplementary Table 4. Coefficients, significance values, and goodness of fit values for the linear mixed-effects models of toughness as shown in Supplemental Figure 6. In all cases, the full model originally included random effects for source animal and fixed effects for log of the blade speed, surface condition, storage time before testing, orientation in the joint, and condyle, with all interaction terms. The model was then reduced by removing insignificant higher-order fixed effects ($p > 0.01$), resulting in the final two-parameter model shown here.